Earth Surface Processes and Landforms
Earth Surf. Process. Landforms (in press)
Published online in Wiley InterScience
(www.interscience.wiley.com) **DOI:** 10.1002/esp.1471

Feedbacks between erosion and sediment transport in experimental bedrock channels

Joel P. Johnson* and Kelin X. Whipple
Department of Earth, Atmospheric and Planetary Sciences, Massachusetts Institute of Technology, Cambridge, MA, USA

**Correspondence to: Joel P. Johnson, Department of Earth, Atmospheric and Planetary Sciences, Massachusetts Institute of Technology, 77 Massachusetts Avenue, Cambridge, MA 02139, USA. E-mail: joelj@mit.edu*

Received 1 March 2006;
Revised 3 November 2006;
Accepted 7 November 2006

Abstract

Natural bedrock rivers flow in self-formed channels and form diverse erosional morphologies. The parameters that collectively define channel morphology (e.g. width, slope, bed roughness, bedrock exposure, sediment size distribution) all influence river incision rates and dynamically adjust in poorly understood ways to imposed fluid and sediment fluxes. To explore the mechanics of river incision, we conducted laboratory experiments in which the complexities of natural bedrock channels were reduced to a homogenous brittle substrate (sand and cement), a single sediment size primarily transported as bedload, a single erosion mechanism (abrasion) and sediment-starved transport conditions. We find that patterns of erosion both create and are sensitive functions of the evolving bed topography because of feedbacks between the turbulent flow field, sediment transport and bottom roughness. Abrasion only occurs where sediment impacts the bed, and so positive feedback occurs between the sediment preferentially drawn to topographic lows by gravity and the further erosion of these lows. However, the spatial focusing of erosion results in tortuous flow paths and erosional forms (inner channels, scoops, potholes), which dissipate flow energy. This energy dissipation is a negative feedback that reduces sediment transport capacity, inhibiting further incision and ultimately leading to channel morphologies adjusted to just transport the imposed sediment load.

Keywords: bedrock channel; erosion; sediment transport; laboratory flume; Henry Mountains, Utah

Motivation

Tectonics and isostasy combine to create positive topography that is eroded and sculpted by surface processes. River networks propagate signals of base level change upstream through incision or aggradation and also move eroded material downstream through sediment transport, making landscapes particularly sensitive to river channel dynamics. Erosion in bedrock channels can respond to changes on human timescales. Anthropogenic effects (e.g. mining, logging, grazing, dam construction and removal, road building) and natural stochastic events (e.g. wildfires, landslides, debris flows) can significantly change short-term sediment fluxes (Roering and Gerber, 2005) and have in some cases increased bedrock erosion rates (James, 2004; Stock *et al*., 2005), affecting riparian habitats and the structural integrity of dams, levees, roads and bridges. At orogenic timescales, a more quantitative understanding of erosion processes is needed to understand the coupling among tectonics, topography and climate, and to rationally interpret signals of external forcing (climate, tectonics) from landscapes (see, e.g., Willett, 1999; Whipple and Tucker, 2002; Hancock and Anderson, 2002; Whipple, 2004).

A variety of models have been proposed to predict the dynamics of river channel erosion into bedrock (see, e.g., Howard and Kerby, 1983; Howard *et al*., 1994; Sklar and Dietrich, 1998, 2004; Whipple and Tucker, 1999, 2002; Stark and Stark, 2001), but data needed to evaluate aspects of competing models is rare (van der Beek and Bishop, 2003; Tomkin *et al*., 2003; Whipple, 2004). Numerical simulations of landscape evolution demonstrate that the details of various bedrock channel erosion models can significantly affect simulated landscape behavior (Whipple and Tucker, 2002; Gasparini *et al*., 2006). Channels that incise into bedrock must also transport the sediment load imposed from upstream because otherwise the channel bed will aggrade. Large shear stress thresholds must be overcome to move

boulders and other coarse sediment typically found in bedrock channels, and a large volume of sediment must be transported through the channel network to erode an entire landscape. Therefore, it is unclear at present whether the factor limiting the ability of bedrock channels to vertically incise tends to be the ability of erosion processes to physically remove pieces of bedrock (detachment-limited end member model, DL) or to transport the sediment supply (transport-limited end member, TL), and what criteria would allow this interpretation to be made (Howard, 1998; Whipple and Tucker, 2002).

Directly linking transport and erosion, Sklar and Dietrich (1998, 2004) proposed a physically based bedrock incision model for abrasion by saltating bedload. In the 'saltation-abrasion model', having too little sediment inhibits erosion because few clasts impact the bed (the 'tools effect'), but having too much sediment causes deposition, shielding the bed and also inhibiting erosion (the 'cover effect'). For given flow conditions the highest erosion rate occurs at the balance point between minimum bed cover and maximum bed impacts. Sklar and Dietrich (2001) validated the tools and cover concepts by experimentally abrading flat rock disks. The saltation-abrasion model suggests that the rate of channel incision into bedrock is always influenced by both bedrock detachment and sediment transport, and therefore that neither transport-limited nor detachment-limited conditions can be entirely met when the channel is incising. In the saltation-abrasion model, TL conditions correspond to complete bed cover with incision rate going to zero. The DL end-member does not directly correspond to any part of the saltation-abrasion model, although low sediment supply and strong bedrock emphasize detachment controls. Another interesting and counterintuitive prediction of the saltation-abrasion model is that at high transport stages ($\tau/\tau_{cr} \gg 1$, where τ is basal shear stress and τ_{cr} is the critical shear stress necessary to initiate sediment motion), erosion rate decreases with increasing shear stress because saltation hop lengths increase more rapidly than particle impact velocities.

Our experimental design was inspired by some predictions and limitations of the saltation-abrasion model. The saltation-abrasion model incorporates flow and sediment transport physics that are satisfyingly quantitative, but this physical rigor comes at the price of several simplifying model assumptions (e.g. planar channel bed, single sediment size) that are rarely met in natural channels. In these experiments we evaluate the planar bed assumption by observing erosional feedbacks that create bed roughness and that in turn influence erosion rates. We focus on understanding the tool-starved end of parameter space (where sediment flux Q_s is significantly smaller than transport capacity Q_c) because (1) tool-starved conditions naturally lead to the development of rough bed topography, (2) saltation-abrasion model predictions are arguably furthest from either transport-limited or detachment-limited model behaviors in this range and (3) Sklar and Dietrich (2002) and Davis *et al.* (2005) explore the behavior of sediment cover effects closer to transport-limited conditions in similar flume experiments. We also demonstrate that at least some sculpted erosional forms (Richardson and Carling, 2005) are robust morphologies that naturally develop in flume settings as well as in the field.

Regardless of whether a river is dominantly alluvial or dominantly bedrock, many feedbacks exist between channel morphology and erosional and depositional processes that limit our ability to predict channel response (see, e.g., Wohl, 1993, 1998; Dietrich *et al*., 2003; Jerolmack and Mohrig, 2005). Many properties of channel morphology and bed state can adjust to imposed conditions, including flow width and depth (for a given discharge), slope, bed roughness, bedrock exposure and sediment size (Leopold and Maddock, 1953; Stark and Stark, 2001; Montgomery and Gran, 2001; Stark, 2006). The functional relationships between these variables are poorly understood, and yet they govern the internal dynamics of fluvial channels. For example, what are the positive and negative feedbacks that set the roughness of eroded bedrock channels, and how does this roughness influence channel slope or width? Field data demonstrate that correlations between channel width and slope can significantly influence calculated parameters such as the reach-averaged bed shear stress (Finnegan *et al*., 2005), and yet causality between variables remains elusive.

While possible feedbacks in the dynamics of bedrock channel incision remain largely unexplored, many prior studies have interpreted the significance of elegant erosional forms (e.g. potholes, flutes, scallops, inner channels) that develop during channel incision into bedrock or cohesive sediment (Alexander, 1932; Wohl, 1993; Zen and Prestegaard, 1994; Wohl *et al*., 1999; Springer and Wohl, 2002). Richardson and Carling (2005) propose a classification scheme for fluvially sculpted bedrock forms. Experimental work has been done to understand the flow and sediment conditions that create erosional morphologies. Of particular relevance, Allen (1971) quantitatively explored feedbacks between stable vortices and particular erosional forms (including flutes, scallops and longitudinal grooves) formed in cohesive mud and rock. Longitudinal grooves and inner channels with undulating walls were the primary erosional morphologies formed by sand abrasion into a cohesive substrate by Shepherd and Schumm (1974) and Wohl and Ikeda (1997). In the latter study erosional morphology changed with bed slope, demonstrating that the formation of sculpted forms does not require substrate heterogeneity, but can also develop simply from the internal dynamics of bedrock channel erosion. The influence of this smaller-scale fluvial sculpting on flow and erosion in the channel as a whole is poorly understood.

As will be shown, erosional morphologies formed in our experiments bear a strong geometric resemblance to a variety of sculpted forms observed in many natural bedrock channels (Richardson and Carling, 2005), including incised ephemeral streams in the Henry Mountains, Utah, USA. Our experimental flume conditions are a good analog

DOI: 10.1002/esp

to this field site because (1) the eolian Navajo Sandstone bedrock is homogeneous and unfractured but weak, similar to the experimental substrate, (2) abrasion is clearly the dominant erosion mechanism in the Navajo Sandstone and (3) the natural channels with comparable erosional forms tend to be small and sediment starved with extensive bedrock exposure. In the present work, we study feedbacks between erosion rate, sediment transport and erosional morphology using laboratory flume data. We explore, at least conceptually, what feedbacks and what level of complexity should be incorporated into channel incision models to better recreate the morphology and dynamic behavior of channel incision.

Methods

We conducted a series of laboratory flume experiments using sediment transported in turbulent flow to abrade brittle synthetic 'bedrock' at the Saint Anthony Falls Laboratory (SAFL), part of the National Center for Earth-Surface Dynamics (NCED). Our experiments focused on sediment-starved conditions expected from theory (Sklar and Dietrich, 2004) to exhibit less rapid erosion at higher transport stages. Following Wohl and Ikeda (1997), bed slope was the main variable that we changed; sediment flux and water flux were primarily held constant.

We used an adjustable slope, non-recirculating flume ~5 m long and 40 cm wide. The erodible substrate ('bedrock') was a 15:1 by weight mixture of sand and Portland cement (type I/II), mixed in a cement mixer and allowed to cure in the flume. Due to time constraints the concrete mixtures were only allowed to cure for approximately 5 days before starting each experiment. Concrete strength increases rapidly at first and most strength is achieved after approximately 28 days. Based on typical logarithmic concrete curing curves (e.g. Nelson, 2003), we estimate that after 5 days the concrete reached roughly 75 per cent of its 28 day compressive strength. Following curing each experiment was completed within ~2 days; the strength may have increased by as much as 5–10 per cent over this time period. Our control of concrete strength within and between runs is relatively poor and would benefit from independent measurements of material properties during the experiments. A new concrete mix was made for each experiment. Although weak, our sand and cement 'bedrock' failed by brittle fracturing. In contrast, the damp cohesive clay and sand mixtures eroded by Shepherd and Schumm (1974) and Wohl and Ikeda (1997) probably failed by plastic shearing, making them less ideal bedrock analogues. Studies of the abrasion of brittle materials (such as glass plates) by microfracturing due to particle impacts find that to first order the rate of erosion should scale inversely with the square of tensile strength (discussed by Sklar and Dietrich, 1998, 2004). Sklar and Dietrich (2001) showed that the scaling between laboratory abrasion rates and tensile strength is consistent between natural lithologies and sand/cement mixtures such as ours, justifying its use as an analog material in erosion experiments.

We conducted five separate flume experiments overall; here we primarily report data from three plane-bed experiments with bed slopes of 2, 5 and 10 per cent, which were the third, second and fourth runs conducted respectively. The first experiment was intentionally an exploratory run using different sediment sizes and fluxes; the initial bed topography (mean slope 5%) was sculpted by hand into a nonuniform surface with several prominent bulges. The next three experiments which we focus on all started with planar bed surfaces. Finally, the bed topography of the fifth flume run was molded with a series of small vertical flume-spanning steps (mean slope 10%). Overall, the first and last experiments showed the same basic feedbacks between erosion and bed topography as the initially planar-bed runs.

A sediment feeder (Tecweigh CR12) distributed fine gravel ($D_{50} = 2{\cdot}50$ mm; $D_{10} = 1{\cdot}68$ mm; $D_{90} = 3{\cdot}76$ mm) at the upstream end of the flume primarily at 68 g/s (245 kg/hr). Sediment fell onto a diffuser to spread it approximately uniformly across the flume width. Water discharge was primarily held constant at 45 L/s, and was continuously monitored at a V-notch weir downstream of the flume. The end of the flume was elevated above the floor, and water jetted off unobstructed. At the downstream flume end the concrete substrate was molded into a vertical step, which eroded down gradually during the experiment. In this manner, baselevel was not fixed artificially but adjusted itself with erosion. Water did not accelerate much as it approached the drop-off at the flume end because flow was supercritical. Because of erosion the flume slope down the axis of the eroded inner channel increased slightly during the flume runs, although bed roughness also increased significantly. Average water velocity was calculated at the beginning of each experiment from flow depth, width and discharge. We have no local velocity measurements as the experiments progressed, so spatial and temporal deviations from the mean sediment and water flow rates were only qualitatively observed.

Flow was supercritical (Table I) with Froude numbers (Fr) from ~1·4 to ~2·5 with increasing flume slope and constant discharge. We acknowledge that this range is higher than is likely common in natural channels, even at flood stage, although Tinkler and Parrish (1998) report field measurements of Fr around 1·7–1·9 for flow along a 40 m reach during a moderate flood in a natural river. They conclude that near-critical, critical and supercritical flows are likely common during floods and that subcritical flow is probably rare along the channel thalweg. Grant (1997) argues that natural channel morphology may adjust to attain $Fr \sim 1$ on average, although this may commonly occur with spatial transitions back and forth between subcritical and supercritical flow. The most appropriate natural comparison to our

DOI: 10.1002/esp

Table I. Summary of initial experimental flow and sediment transport conditions at the beginning of each experiment. We do not have velocity measurements once erosional topography developed. A flume width of 40 cm with a rectangular cross section was used in calculations. Flow depth was measured at the beginning of the 5 and 10 per cent slope experiments when the bed was planar, and mean velocity was calculated from this and the discharge, continuously monitored at a weir. Flow depth was inadvertently not measured at 2 per cent slope, and so a flow depth was calculated for this experiment using a range of Manning's *N* values suggested by Manning's *N* values calculated from the other experimental runs. Mean shear stress and sediment transport capacity were calculated using the depth–slope product (including hydraulic radius, width 0·4 m), sediment flux $Q_s = 0{\cdot}068$ kg/s, nondimensional critical shear stress $\tau^*_{cr} = 0{\cdot}03$ and the bed load sediment transport equation given by Fernandez Luque and van Beek (1976, presented by Sklar and Dietrich, 2004)

Mean slope	2 per cent	5 per cent	10 per cent
Manning's N	0·18–0·02, estimated	0·019	0·021
Flow depth, cm	8–9, calculated	6·8 (6–7)	5·7
Mean velocity, calculated, m/s	1·3–1·2	1·6	1·9
Froude number	1·3–1·5	1·9	2·5
τ, Pa, calculated	12	25	44
τ^*, calculated	0·32	0·68	1·2
Trans. stage, τ^*/τ^*_{cr}	11	23	39
Q_c, trans. cap, kg/s	0·42	1·4	3·4
Q_s/Q_c	0·16	0·048	0·020

high *Fr* experiments may be over steps and steep reaches where bedrock is most exposed and abrasion (where applicable) most clearly a rate limiting process. Shepherd and Schumm (1974) report *Fr* between 0·66 and 1·02 for their erosion experiments, while Wohl and Ikeda (1997) reached *Fr* between 1·1 and 1·6. Erosional morphologies and the formation of inner channels in their experiments were similar to ours, suggesting *Fr* sensitivity may be minor. Future work should explore the sensitivity of our results to *Fr*; it is possible that standing waves, hydraulic jumps and changes in shear stress associated with transitions about $Fr \sim 1$ could be significant in focusing erosion.

Surface topography of the eroding bed was quantitatively measured from photographs taken with a Nikon D100 digital camera oriented 45 degrees from a vertical line laser (Figure 1). The oblique images were corrected for perspective distortion and the red laser lines that defined cross-stream topographic swaths were automatically extracted using Matlab image processing techniques (Kovesi, 2000). We estimate the uncertainty on the elevation measured at each location to be ±1 mm at 95 per cent certainty (two standard deviations). We profiled a 3 m long, 30 cm wide stretch of the flume at a downstream spacing of 3 cm and cross-stream spacing of 0·25 mm. The narrow tortuous grooves that developed caused significant data dropouts due to obstructed views of the line laser. The amount of erosion in a given timestep is known by differencing sequential topographic maps. Complete experiments lasted 7–9 hours of run time, with surface topography measured at intervals between 30 and 60 minutes (Table II).

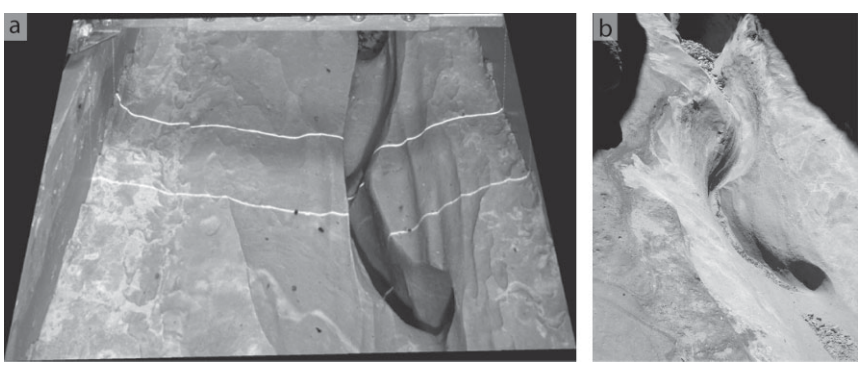

Figure 1. (a) Erosional morphology during the 10 per cent slope experiment, looking upstream. The trapezoidal photograph shape of the picture is a correction for oblique distortion. The two bright lines are from red vertical sheet lasers, which are extracted to give quantitative measurements of cross-section topography. Flume width 40 cm. (b) This small natural inner channel incised into Navajo Sandstone in the Henry Mountains Utah has a similar morphology. Field of view ~ 1·5 m.

DOI: 10.1002/esp

Table II. Water discharge and sediment flux of each sequential timestep for which topography was measured. In order to roughly compare timesteps with different sediment fluxes, we calculated what the 'effective' timestep duration at 68 g/s sediment flux would be by assuming a linear relationship between sediment flux and erosion. For example, Q_s = 122 g/s for 30 minutes corresponds to (122/68) × 30 = 54 minutes effective run time. In the 5 per cent slope experiment the initial two time periods at low water discharge were not included in the effective timestep calculations, as the bed aggraded with negligible erosion. Most timesteps are directly comparable. Note that erosion rate (cm/hr) is plotted in Figure 4, rather than erosion depth (cm) given here. Mean erosion in each timestep was calculated over a flume width of 30 cm. Inner channel erosion was calculated over a 1 cm wide swath chosen by eye in each timestep to follow the developing and migrating inner channel

Timestep	Duration (min)	Q_w (L/s)	Q_s (g/s)	Erosional interface width (cm)	Mean erosion depth (cm)	Inner channel mean erosion depth (cm)
2% slope						
1	40	43	68	0·10	0·12	0·26
2	50	43	68	0·20	0·16	0·46
3	50	43	68	0·31	0·16	0·46
4	50	43	68	0·42	0·14	0·49
5	40	43	68	0·46	0·08	0·32
6	40	43	68	0·53	0·10	0·44
7	60	43	68	0·64	0·15	0·67
8	60	43	68	0·74	0·12	0·56
5% slope						
	5	7·5	68			
	14	7·5	122			
	30	43	122			
1, effective	***54***	***43***	***68***	0·40	0·37	1·28
2	30	43	68	0·64	0·21	1·12
3	30	43	68	0·85	0·18	1·25
4	30	43	68	1·02	0·16	0·93
5	30	43	68	1·15	0·12	0·65
6	30	43	68	1·26	0·12	0·59
7	60	43	68	1·40	0·23	0·78
8	60	43	68	1·54	0·19	0·88
9	60	43	68	1·80	0·16	0·88
10a	30	43	122			
10b	2·5	43	14			
10c	2	43	27			
10d	1·5	43	41			
10e	2	43	54			
10f	2	43	68			
10g	2·5	43	81			
10h	1	43	95			
10, effective	***64***	***43***	***68***	1·98	0·15	0·76
10% slope						
1a	4	43	122			
1b	37	43	68			
1, effective	***44***	***43***	***68***	0·16	0·24	0·45
2	45	43	68	0·39	0·25	0·91
3	43	43	68	0·64	0·23	1·07
4	45	43	68	0·89	0·24	1·25
5	45	43	68	1·06	0·22	0·94
6	45	43	68	1·25	0·16	0·96
7	45	43	68	1·43	0·14	0·98
8	45	43	68	1·61	0·13	0·90
9	45	43	68	1·75	0·12	0·89
10	45	43	68	1·96	0·12	0·98

DOI: 10.1002/esp

As Figure 1 indicates, the flume bed did not remain planar but eroded to form significant topography. We characterize the rough topography at a given timestep as an 'interface width' w, a metric used to quantify changes in average surface roughness (Barabási and Stanley, 1995):

$$w(N,t) = \sqrt{\frac{1}{N}\sum_{i=1}^{N}[h(i,t) - \bar{h}(t)]^2}$$

where t is time, i is a spatial index, N is the total number of measurements, h is the surface height at a given location and time and the overbar represents a spatial average. Note that w is simply the standard deviation of surface elevations at a given timestep, making it an intuitive measure of how much elevation varies about the mean elevation. To compare different experiments we subtracted the initial, approximately planar surface of each experiment from sequential eroded surfaces so that w starts at zero when comparing different experiments.

Results

Figure 2(a)–(d) shows cumulative erosion depth in several sequential timesteps starting with a plane bed at 10 per cent slope. As the bed topography evolved we observed corresponding changes in the spatial distribution of transported sediment. Sediment entered the channel, uniformly distributed across the width, ~50 cm upstream of the upstream end of the topography map. In the initial timestep (2(a), 44 min run time) erosion was broadly distributed across the width of the plane bed channel. Sediment was similarly distributed across the channel width and moved as energetic bedload. By the second timestep (2(b), 90 min), a gently sinuous incised groove with semi-periodic lows approximately 25–40 cm apart ran most of the downstream length of the flume. Bedload became focused in these topographic lows, presumably due to gravity, flow convergence and higher flow velocities. For the remaining ~6 hours of the flume run, erosion was primarily focused in this inner channel (2(c), 2(d)) because of the positive feedback between the evolving topography and sediment channelization. Most sediment hugged the inner channel bed, although local suspension occurred in stable turbulent eddies. No deposition was observed. At 10 per cent slope a single incised inner channel formed (2(d)), whereas at 5 per cent slope (2(e)) a dominant inner channel developed but with more secondary transport pathways and local lows. Incision progressed more slowly at 2 per cent slope (2(f)); when the run was stopped an inner channel had developed in the downstream half of the flume, but erosion was distributed relatively broadly over the flume width. Later timesteps at 2 per cent slope looked similar to earlier, less incised timesteps at both 5 and 10 per cent slope.

By the end of the experiments at 5 and 10 per cent slope, the tortuous inner channels had undulating walls (Wohl, 1998; Wohl *et al*., 1999) and tight lateral bends including dramatic undercuts. In addition to inner channels we saw scoops, wall undulations and potholes that morphologically match those seen in many natural bedrock channels, particularly in the Henry Mountains, Utah (Figures 1 and 3). The geometric similarity between a variety of field and flume sculpted forms suggests that the laboratory experiments are reasonable recreations of at least some aspects of natural channel abrasion. Figure 3(a), (b) compares flume and field inner channels. Note the local highs and lows in bed elevation along the inner channel. Figure 3(c) shows erosion around an initial bulbous mound molded into the flume bed of the first (exploratory) flume run. Water flowed over the top of the mound; the bed-hugging sediment bifurcated around the mound, following the horseshoe flow vortex and preferentially eroding the bottom and sides. Figure 3(d) shows similar geometry of a trough presumably sculpted by a horseshoe vortex around a protrusion in a Henry Mountains channel. Arrows point to two of seven bolts that we are currently using to monitor erosion (Johnson *et al*., 2005).

Potholes in both natural channels and our experiments often have spiral grooves down the sides (Alexander, 1932; Zen and Prestegaard, 1994; Wohl, 1993; Hancock *et al*., 1998; Whipple *et al*., 2000; Springer and Wohl, 2002; Springer *et al*., 2005). Figure 3(e), (f) shows two views from above of a 5–6 cm diameter flume pothole. By the timestep shown the pothole had eroded to the flume bottom. Note the spiral grooves down the inside. In comparison, Figure 3(g) shows a natural pothole with similar incised inlet and outlet grooves. Figure 3(h) shows a ~2 m diameter natural pothole with spiral grooves down the inside. In our experiments, potholes were eroded by sediment that entered as bedload but then became locally suspended by the upward-directed flow exiting the pothole. No static sediment accumulated in potholes. Potholes formed in the 10 per cent slope experiment but not at 5 or 2 per cent slopes. Once formed, potholes were erosionally significant: in one timestep, the approximate erosion rate at the bottom of one pothole (diameter 5–6 cm, eroded depth 7 cm in <45 minutes) was 50 times larger than the flume average, or ~1/5 of the measured volume eroded from the rest of the flume.

DOI: 10.1002/esp

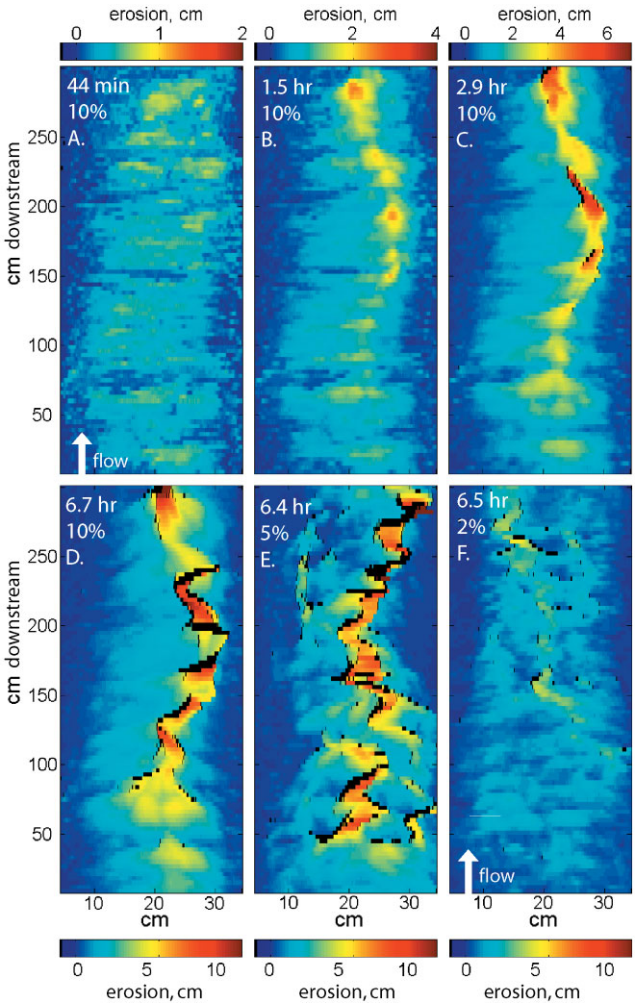

Figure 2. Cumulative erosion depth since beginning of experiment. See text for descriptions. Flow is from bottom (0 cm) to top (250+ cm). Note differences in color-bar scaling between plots. Data dropouts are black (no data). The middle 30 cm of the 40 cm flume width is shown. (a) 10 per cent slope, run time 44 minutes. (b) 10 per cent slope, 90 minutes total run time. (c), (d) 10 per cent slope, after 2·9 and 6·7 hours of total run time respectively. (e) 5 per cent slope, 6·4 hours of run time. (f) 2 per cent slope, 6·5 hours of run time.

Erosion rates progressed differently at 2, 5 and 10 per cent slopes. Figure 4(a) shows that interface width increases monotonically with run time, because the topographic lows erode while the upper surface remains less incised. As relief and roughness increased from the starting plane-bed condition, average flume-wide vertical erosion rates decreased (Figure 4(b)). However, when erosion is averaged only over a 1 cm wide swath that follows the shifting zone of focused erosion (the developing inner channel), a somewhat different picture emerges (Figure 4(c)): at 5 and 10 per cent initial plane-bed slope, erosion rates in the first several timesteps increased in the zone of focused erosion as sediment was channelized by topography into a narrower and deeper zone. As focused incision continued the inner slot narrowed, and erosion rates decreased and then stabilized in response to locally increasing sediment flux and flow resistance.

Figure 5(a) shows the progression of erosion and variable bed topography in sequential timesteps of a 10 per cent slope channel cross-section. Erosion is broadly distributed initially but becomes focused in an inner channel. Local lows tend to preferentially erode faster. Figure 5(b) shows that the eroding bottom topography at 10 per cent slope developed semi-periodic lows that migrated downstream. The amplitude of the topography grows consistently during the experiment as focused incision forms an inner channel. Note the overall downstream migration of areas with focused erosion. The downstream migration rates of the topographic lows are approximately 2·5–4 cm/hr, somewhat faster than the vertical incision rates (Figure 4(b), (c)).

DOI: 10.1002/esp

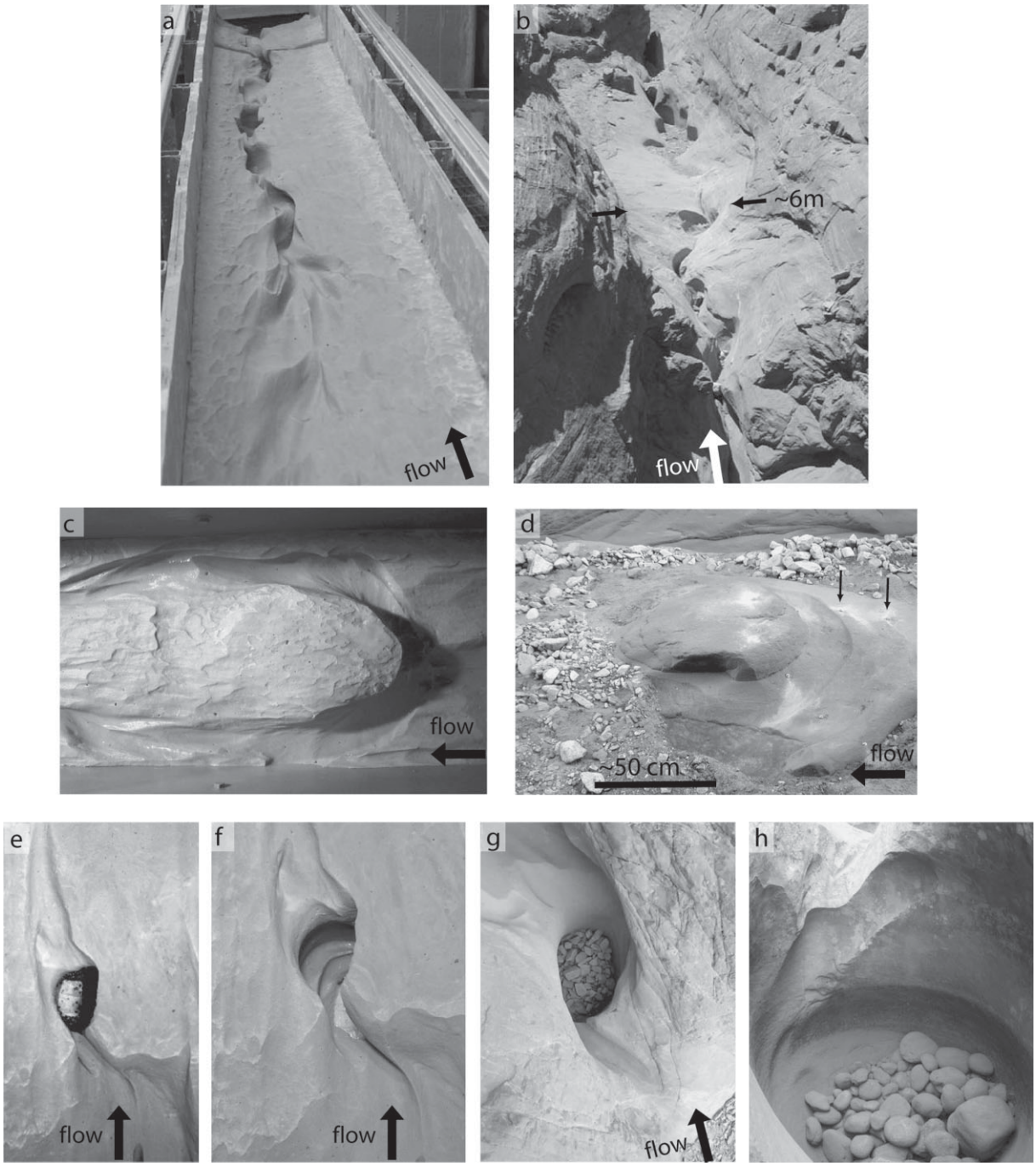

Figure 3. Comparisons of erosional features formed in flume and field. All the field photographs are channels and canyons draining the Henry Mountains of Utah that have incised into the relatively weak but unfractured Navajo Sandstone. (a) Oblique view looking downstream at the end of the 10 per cent slope flume experiment. Compare with 2(d). Flume width 40 cm. (b) A natural inner channel formed in the south fork of Maidenwater Creek. (c) View from above of experimental erosion around a broad protrusion molded into the bed of the first flume run. Flume width 40 cm. (d) Similar geometry of a trough in a Henry Mountains channel, initial condition unknown. White patches are pulverized rock from drilling bolt holes for erosion monitoring. (e), (f) Two views of a pothole formed in the fifth flume run in which the bed was molded to have vertical steps; the pothole occurred where the bed was initially horizontal and planar. Pothole diameter 5–6 cm; overall bed slope 10 per cent. (g) Field pothole (diameter ~ 60 cm) partially filled with sediment clasts. (h) Natural pothole, diameter ~2 m. This pothole is from the cascade of potholes shown in Figure 2 of Whipple (2004).

DOI: 10.1002/esp

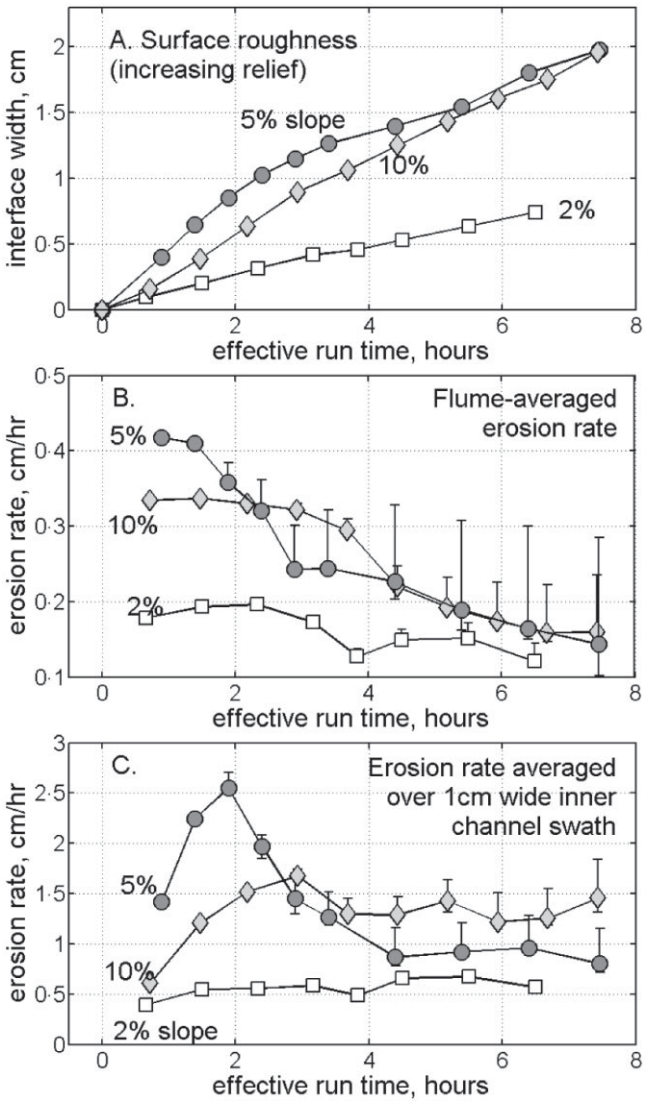

Figure 4. Surface roughness and erosion. (a) Interface width plotted against effective run time (Table I). (b) Erosion rates for each timestep averaged over the measured flume area (30 cm wide by 300 cm long). The asymmetric uncertainty is primarily due to the data dropouts in the measured timestep topography, and the error bars represent minimum and maximum possible amounts of erosion given that few dropout locations eroded to the flume bottom by the end of the run. Most erosion by potholes unfortunately is not included because our method for measuring topography could not see the pothole bottoms. (c) Inner channel erosion rate calculated over a 1 cm wide by 300 cm long swath. The location of the 1 cm zone was chosen by eye to follow the path of highest erosion, and shifted between timesteps as the inner channel developed and migrated.

Interpretations

As documented above, patterns and rates of erosion depend on feedbacks between flow, topography and sediment transport. Only when the bed was initially planar did sediment remain broadly distributed across the channel width. Bed topography, flow convergence and gravity channelize sediment into interconnected and eroding local lows causing the *local* sediment flux to increase, while the local sediment transport capacity decreases due to increased flow resistance in the developing inner channel. Local erosion rate clearly depended on the local sediment flux. We qualitatively interpret the increase and then decrease in inner channel erosion rates (Figure 4(c)) to reflect first tools and then cover effects (Sklar and Dietrich, 1998, 2004), with increasing and decreasing erosional efficiency as the

DOI: 10.1002/esp

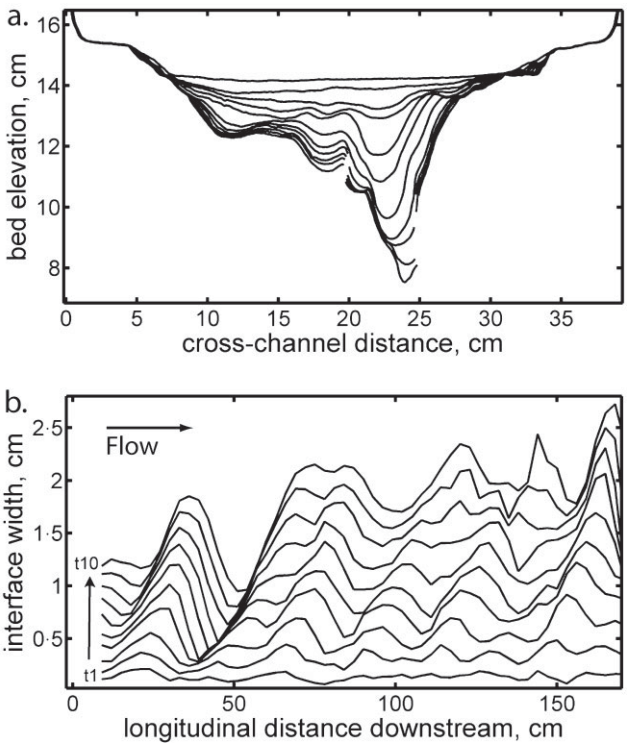

Figure 5. Measurements of sequential erosional topography at 10 per cent slope. (a) Sequential timesteps for a single flume cross-section at approximately 204 cm in Figure 2(a)–(d). (b) Interface width (Equation (1)) at each flume cross section plotted against time. Shown here is the upstream half of the flume; downstream in this experiment (10% slope) the inner channel became too incised to obtain accurate interface widths at every cross section due to significant overhangs and undercuts. We are unsure of what sets the wavelength.

local ratio of sediment flux to transport capacity (Q_s/Q_c) increases. The saltation-abrasion model uses width-averaged values of transport capacity and sediment flux. For a given discharge and sediment flux it predicts a single erosion rate, in contrast to our observations (Figure 4(b), (c)). Slope and partial bed cover are two degrees of freedom for channel response explicitly incorporated into the saltation-abrasion model. However, the saltation-abrasion model assumes plane bed geometry, and so does not incorporate the morphological degree of freedom that leads to significant erosion rate changes in these experiments.

An intriguing prediction of the saltation-abrasion model is that erosion rates will drop at high shear stresses (when all else is held equal, as in our experiments) because the modest increase in vertical impact velocity with increasing shear stress does not compensate for the decreasing number of particle impacts per area as the saltation hop length also increases. The initial rate of focused incision is greater at 5 per cent slope than at 10 per cent slope, which may be consistent with this hypothesis (Figure 4(b), (c)). For the average sediment transport conditions calculated at the beginning of the experiments (Table I), the saltation-abrasion model does predict higher erosion rates at 5 per cent slope than at 10 per cent slope, but also predicts the highest erosion rates at 2 per cent slope, in contrast to our observations. This is true whether or not suspension effects are included in the saltation-abrasion model calculations (Sklar and Dietrich, 2004).

Topographic controls on flow and sediment transport

The decline in erosion rate at high shear stress predicted by the saltation-abrasion model may not apply once significant bed topography has developed. We interpret that the developing bed topography influenced flow, sediment transport and erosion in several ways. First, rough bed topography changes the flow field. Evolving bed topography and channel morphology (slope, width etc.) control the spatial and temporal distribution of local shear stress (see, e.g., Stark, 2006). The increased roughness from sculpted forms is likely to reduce the local shear stress in the zone of active sediment transport and erosion, due to increased form drag (Wohl and Ikeda, 1997; Wohl, 1998; Wohl *et al*.,

DOI: 10.1002/esp

1999). This would reduce the sediment transport capacity of the local flow. We emphasize that we did not make any measurements of changes in flow resulting from rough topography; we only infer this likely feedback between flow and topography.

Second, rough topography controls the spatial distribution of sediment transport. Patterns of abrasion will not match patterns of shear stress because flow expends energy through friction on the sidewalls but abrasion only occurs where sediment impacts the boundary. Sediment becomes focused in local topographic lows because of lateral slope-dependent transport due to gravity. Initially in our experiments the bed was nearly planar and so lateral transport was weak, but early timesteps still demonstrate preferential erosion of lows, which gradually become interconnected by erosion. Sediment is dominantly transported downstream, and so the local sediment flux depends on the upstream bed topography and sediment transport field. The relationship between bed shear stress and erosion rate is an explicit function of the sediment transport field, which is in turn mediated in complex ways by the evolving bed topography. Additional feedbacks can also occur between erosion and sediment transport; Davis *et al.* (2005) conducted similar flume experiments over a wider range of average Q_s/Q_c. They found that higher relative supply produced less eroded roughness for initially planar beds, but had the opposite effect on initially rough beds because sediment deposited in the topographic lows and erosion only attacked higher exposed points.

Third, rough topography controls the energetics of sediment impacts. Once developed, the frequency of particle impacts will probably scale with various aspects of the bed topography rather than with the saltation hop length as assumed in the saltation-abrasion model. For example, tight curves along the tortuous inner channel (Figures 2(d), (e) and 3(a)) lead to spatial accelerations of both flow and sediment, focusing abrasion on the outside walls of bends. The quasi-periodic topographic lows shown in Figure 5 are another example of topographic control on sediment impacts. The downstream translation of the local lows indicates preferential abrasion on upstream faces. Energetically, sediment grains will often impact the boundary at velocities far exceeding the settling velocity, especially when incipiently suspended. Visual observations suggest that the most erosive conditions in our experiments (e.g. pothole formation) occurred when the sediment, primarily traveling as bedload, became incipiently suspended by local turbulent flow conditions. In the 10 per cent slope experiment potholes formed suddenly once the eroding topography created a vertically oriented stable vortex in the flow. In contrast, at 5 per cent slope tortuous flow conditions in the inner channel led to complex patterns of three-dimensional erosion, but never formed stable vertical vortices or potholes. We suspect that at 10 per cent slope a threshold had been exceeded due to local topography, flow and incipient sediment suspension, allowing the potholes to form and greatly enhancing the local erosion rate, consistent with field observations (Whipple, 2004; Barnes *et al*., 2004).

The saltation-abrasion model was intentionally constructed to represent bedload impacts only, and so erosion decreases to zero in the model as sediment grains approach the threshold of suspension. Previous studies have often inferred that the complex geometries and sharply eroded edges of sculpted morphologies such as flutes and potholes require tight coupling between flow vorticity and sediment transport, and therefore imply that suspended sediment rather than bedload is responsible for the erosion (Alexander, 1932; Wohl *et al*., 1999; Whipple *et al*., 2000). While this interpretation is probably correct, the suspension need only reflect *local* turbulent conditions, not width- or reach-averaged values. If one were to calculate the mode of transport for different sediment size classes using width-averaged parameters such as the mean shear stress, the smaller end of the bedload class would be most likely to become incipiently suspended by local turbulence. A testable hypothesis is that impacts from sediment incipiently suspended by stable flow vortices are the most erosive, i.e. remove the most material per impact or per unit mass of sediment in that size class.

Transport-limited bed morphology

In our experiments, the channel apparently evolved towards a transport-limited bed morphology. We qualitatively tested this hypothesis in the 5 per cent slope experiment: a small increase in sediment feed rate led to rapid static alluviation of the inner channel, while a small decrease in sediment feed rate led to renewed inner channel incision of an even narrower slot. The entire channel could transport more sediment, so the entire channel is not at its transport capacity, but in our experiments the fraction of channel actually transporting sediment (i.e. the inner channel) approached transport-limited conditions rather quickly. Shepherd and Schumm (1974) and Wohl and Ikeda (1997) observed sediment deposition in their experimentally eroded inner channels, suggesting that erosion in their experiments also led to transport-limited conditions. Erosional bedforms and undulating canyon wall morphologies dissipate flow energy (Wohl and Ikeda, 1997; Wohl, 1998; Wohl *et al*., 1999) and are probably key components in reaching transport-limited conditions. In spite of suggestions of transport-limited conditions in our experiments, erosion rate never went to zero in the inner channel (Figure 4(c)) as predicted by the saltation-abrasion model for $Q_s/Q_c \sim 1$. This may indicate that the formulation of the cover effect is incomplete in the saltation-abrasion model. In our experiments,

DOI: 10.1002/esp

abrasion may have continued intermittently under a coherent carpet of moving sediment, or intermittent suspension and locally focused erosion in the tortuous inner channel may account for erosion rate not dropping to zero and varying with flume slope.

Our experiments suggest that sediment cover effects may become dominant at even lower ratios of width-averaged sediment flux to sediment transport capacity (Q_s/Q_c) than the saltation-abrasion model predicts. Sklar and Dietrich (2004, 2006) suggest that most incising channels may be in the cover-dominated side of parameter space. Based on the feedbacks we find, it is plausible that the first-order behavior of a wide range of incising bedrock channels is even closer than they infer to the cover end-member of the saltation-abrasion model where channels behave as transport limited, even in cases where erosional morphologies are dramatic and channels appear sediment starved.

Inner channel formation and channel width controls

Inner channel formation can naturally result from the positive feedbacks we describe between sediment transport, erosion and topography that focus local incision. Along an Australian bedrock channel with variable erosional morphologies, Wohl (1993) documented that inner channel locations correlated with higher channel gradients, consistent with the feedback we propose. In general, inner channels may often indicate low sediment load relative to the width-averaged transport capacity of the flow – i.e. sediment-starved conditions. Further study may allow flow and sediment transport conditions to be constrained from specific erosional forms (Allen, 1971; Zen and Prestegaard, 1994; Richardson and Carling, 2005).

Inner channel development also gives insight into width controls of bedrock channels – if incision had continued indefinitely, all of the sediment and flow would eventually have been contained in the narrow slot. Inner channel width in our experiments seemed to increase with increasing Q_s/Q_c, although focused undercutting and bed topography in the inner channel makes it hard to definitively pick out width relations from these data. A testable hypothesis is that bedrock channel width is a dominant component of the morphological adjustment towards transport-limited conditions ($Q_s/Q_c \sim 1$). As such, width should decrease with increasing slope if sediment flux remains the same (e.g. if it is limited by the supply from a lower slope reach upstream) but shear stress and transport capacity increase, qualitatively consistent with the slope–width scaling of Finnegan *et al.* (2005).

Our experiments show that the evolving erosional morphology of the channel boundary can significantly affect erosion rates. Acknowledging that channel adjustment involves more than just vertical incision and slope changes, Stark and Stark (2001) lumped the dynamic factors that collectively define channel morphology into a variable called *channelization*, which abstractly 'represents the ease with which sediment can flux through a channel reach'. In their model, a local channel reach is equilibrated when its slope and channelization value combine to just transport the local sediment flux. Our results are consistent with this approach. However, the channelization parameter does not define any functional relationships between the relevant components of channel morphology. Understanding the sediment flux and channel slope relations that lead to inner channel formation are a step in this direction.

Experimental idealizations and natural channel complexity

Our idealized experiments intentionally neglect many complexities, including other erosion processes (e.g. hydraulic plucking), higher sediment fluxes, a broad distribution of sediment sizes and a wide distribution of flow magnitudes. These factors may explain a broader range of observable channel morphologies in actively incising landscapes, but may also limit the strength of expression of our proposed feedbacks in natural channels. Our hope with this work is to document and understand basic feedbacks between erosional topography and sediment transport under conditions where the feedbacks are expressed most prominently (single constant discharge, sediment flux and sediment size). These same feedbacks between channel morphology and erosion should still exist in all channels even if they are sometimes overwhelmed by additional complexities and local conditions. For example, bedrock will rarely if ever be able to erode quickly enough to reach a transport-limited morphology during floods, although patterns of erosion will at least tend in that direction. Quick and complementary bed adjustments can also occur by sediment entrainment and deposition. Natural channel morphology will always represent an amalgamation of discharge and sediment transport magnitudes and durations.

The importance of variable flood discharge will be closely connected to the size distribution of sediment available for transport into and through the channels. The largest floods are likely responsible for transporting the coarsest sediment that becomes immobile at lower flows (e.g. Howard, 1998), armoring the bed. Coarse sediment is often the dominant bed roughness element, rather than *in situ* bedrock. In large, actively incising channels such as the Indus River (Hancock *et al*., 1998; Whipple *et al*., 2000) boulders often erode in place, presumably until they are small enough to be transported in a flood. Field observations of bedrock channels and canyons in many places (e.g., Wohl,

DOI: 10.1002/esp

1992; Howard, 1998; Massong and Montgomery, 2000; Barnes *et al*., 2004; Johnson *et al*., 2005) show that inner channels and entire 'bedrock' channels are often choked with coarse sediment, especially boulders. Sklar and Dietrich (2002) conducted flume experiments with coarser sediment in channels close to transport capacity, to explore transitions between bedrock exposure and sediment cover. In their experiments, an inner groove began to incise where sediment transport was focused, but sediment then deposited in these subtle topographic lows, showing that deposition is also sensitive to local topography. A wide distribution of flood magnitudes and sediment sizes may spread erosion more broadly across the entire channel width rather than focusing into a narrow inner channel as in our sediment-starved case.

Future experimentation should further explore details of the feedbacks we suggest here, focusing on quantifying changes in local sediment flux and flow rate as the topography develops. In addition, relations between developing bed roughness, erosion rate and slope should be explored further. We are hesitant to push the comparisons between experiments too far in this preliminary data set because of uncertainties including concrete strength between runs, topographic data dropouts in the inner channel and exact flow conditions. Specific predictions of the saltation-abrasion model, such as decreases in erosion rate explicitly tied to changes in saltation hop lengths, should be explored. Future experimental work should also systematically explore parameter space with ranges of flow discharges, relative sediment supply (Q_s/Q_c), sediment sizes and Froude numbers. We hope to address some of these questions in ongoing flume experiments. The saltation-abrasion model explicitly incorporates changes in bed cover in a physically reasonable way; more accurate models of incision will require a better understanding and parameterization of additional internal dynamics (i.e. width, roughness, slope, erosion) of fluvial channels.

Conclusions

When the transport capacity of flow in a channel is greater than the sediment load, the nonuniform distribution of sediment impacts leads to nonuniform abrasion. In our experiments, both the mean and distribution of erosion rates change as the bed topography evolves, even with constant water and sediment discharges. Bed topography is thus a degree of freedom for bedrock channel response that mediates (1) the flow structure and local turbulent intensity, (2) the spatial distribution of sediment impacts on the bed and (3) the rate and spatial distribution of fluvial erosion. We find evidence to support both tools and cover effects of abrasion by transported sediment, confirming the central hypothesis of Sklar and Dietrich (1998, 2004), but in response to *local* sediment flux and shear stress, not width- or reach-averaged values.

Bed topography is the dominant control on sediment impact location and intensity once significant erosional relief develops. The relation between shear stress and erosion rate is non-unique, and may vary significantly between different sculpted erosional morphologies. Potholes in particular are extremely efficient erosive agents when they develop. Inner channels may indicate reach-averaged sediment starved conditions (low Q_s/Q_c) that lead to a spatial focusing of sediment transport and erosion. While natural variability (e.g. a wide distribution of flood discharges and sediment sizes) may obscure the expression of the proposed feedbacks in field settings, we suggest that bedrock channel roughness, often expressed as dramatic sculpted morphologies, tends to increase in amplitude until enough turbulent energy is dissipated by form drag that the flow just transports the sediment load. Our experiments suggest that transport-limited conditions may sometimes occur even in sediment-starved channels with negligible bed cover and dramatic, active erosional morphologies.

Acknowledgements

Leonard Sklar, Douglas Jerolmack and David Mohrig are great sources of ideas on channel dynamics. Thanks to Jeff Marr at SAFL for invaluable help designing and preparing the experimental setup, as well as Gary Parker and Chris Paola. This work was supported by NCED while KXW was on sabbatical at SAFL, and by NSF Geomorphology and Land Use Dynamics and Hydrological Sciences grants EAR-0439037 and EAR-0345622. We thank Leonard Sklar and Colin Stark for constructive comments and Ellen Wohl for reviewing an earlier version of this manuscript.

References

Alexander HS. 1932. Pothole erosion. *Journal of Geology* **40**: 305–337.

Allen JRL. 1971. Transverse erosional marks of mud and rock: their physical basis and geological significance. *Sedimentary Geology* **5**: 165–385.

Barabási AL, Stanley HE. 1995. *Fractal Concepts in Surface Growth*. Cambridge University Press: Cambridge.

Barnes CM, Sklar LS, Whipple KX, Johnson JP. 2004. Periodic spacing of channel-spanning potholes in Navajo Sandstone, Henry Mountains Utah: implications for propagation of incision pulses across tributary junctions. *Eos Transactions AGU* **85**(47) Fall Meeting Supplement: Abstract H53C-1276.

Davis JR, Sklar LS, Demeter GI, Johnson JP, Whipple KX. 2005. The influence of bed roughness on partial alleviation in an experimental bedrock channel, *Eos Transactions AGU* **86**(52) Fall Meeting Supplement: Abstract H53D-0508.

Dietrich WE, Bellugi DG, Sklar LS, Stock JD, Heimsath AM, Roering JJ. 2003. Geomorphic transport laws for predicting landscape form and dynamics. In *Prediction in Geomorphology*, Wilcock P, Iverson R (eds), American Geophysical Union Geophysical Monograph 135: 103–132.

Fernandez Luque R, van Beek R. 1976. Erosion and transport of bed-load sediment, *Journal of Hydraulic Research* **14**: 127–144.

Finnegan NJ, Roe G, Montgomery DR, Hallet B. 2005. Controls on the channel width of rivers: implications for modeling fluvial incision of bedrock. *Geology* **33**: 229–232.

Gasparini NM, Bras RL, Whipple KX. 2006. Numerical modeling of non-steady-state river profile evolution using a sediment-flux-dependent incision model. In *Tectonics, Climate and Landscape Evolution*, Willet SD, Hovius N, Brandon MT, Fisher DM (eds), Geological Society of America Special Paper 398: 434.

Grant GE. 1997. Critical flow constrains flow hydraulics in mobile-bed streams: a new hypothesis. *Water Resources Research* **33**: 349–358.

Hancock GS, Anderson RS. 2002. Numerical modeling of fluvial strath-terrace formation in response to oscillating climate. *Geological Society of America Bulletin* **114**: 1131–1142.

Hancock GS, Anderson RS, Whipple KX. 1998. Beyond power: bedrock river incision process and form. In *Rivers Over Rock: Fluvial Processes in Bedrock Channels*, Tinkler K, Wohl EE (eds), American Geophysical Union Geophysical Monograph **107**: 35–60.

Howard AD. 1998. Long profile development of bedrock channels; interaction of weathering, mass wasting, bed erosion, and sediment transport. In *Rivers Over Rock: Fluvial Processes in Bedrock Channels*, Tinkler K, Wohl EE (eds), American Geophysical Union Geophysical Monograph 107: 237–260.

Howard AD, Dietrich WE, Seidl MA. 1994. Modeling fluvial erosion on regional to continental scales. *Journal of Geophysical Research-Solid Earth* **99**: 13 971–13 986.

Howard AD, Kerby G. 1983. Channel changes in badlands. *Geological Society of America Bulletin* **94**: 739–752.

James LA. 2004. Tailings fans and valley-spur cutoffs created by hydraulic mining. *Earth Surface Processes and Landforms* **29**: 869–882.

Jerolmack D, Mohrig D. 2005. Interactions between bed forms: topography, turbulence, and transport. *Journal of Geophysical Research – Earth Surface* 110.

Johnson JP, Whipple KX, Sklar LS. 2005. Field monitoring of bedrock channel erosion and morphology. *Eos Transactions AGU* **86**(52) Fall Meeting Supplement: Abstract H52A-01.

Kovesi PD. 2000. *MATLAB and Octave Functions for Computer Vision and Image Processing*. School of Computer Science and Software Engineering, The University of Western Australia. http://www.csse.uwa.edu.au/~pk/research/matlabfns/ [2003].

Leopold LB, Maddock T. 1953. *The Hydraulic Geometry of Stream Channels and Physiographic Implications*, US Geological Survey Professional Paper Report P 0252.

Massong TM, Montgomery DR. 2000. Influence of sediment supply, lithology, and wood debris on the distribution of bedrock and alluvial channels. *Geological Society of America Bulletin* **112**: 591–599.

Montgomery DR, Gran KB. 2001. Downstream variations in the width of bedrock channels. *Water Resources Research* **37**: 1841–1846.

Nelson PK. 2003. *Handbook of Nondestructive and Innovative Testing Equipment for Concrete*, final report. Federal Highway Administration: Washington, DC.

Richardson K, Carling PA. 2005. *A Typology of Sculpted Forms in Open Bedrock Channels*, Geological Society of America Special Paper 392.

Roering JJ, Gerber M. 2005. Fire and the evolution of steep, soil-mantled landscapes. *Geology* **33**: 349–352.

Shepherd RG, Schumm SA. 1974. Experimental study of river incision. *Geological Society of America Bulletin* **85**: 257–268.

Sklar L, Dietrich WE. 1998. River longitudinal profiles and bedrock incision models: stream power and the influence of sediment supply. In *Rivers Over Rock: Fluvial Processes in Bedrock Channels*, Tinkler K, Wohl EE (eds), American Geophysical Union Geophysical Monograph 107.

Sklar LS, Dietrich WE. 2001. Sediment and rock strength controls on river incision into bedrock. *Geology* **29**: 1087–1090.

Sklar LS, Dietrich WE. 2002. Thresholds of alluviation in an experimental bedrock channel and controls on rates of river incision into bedrock. *Eos Transactions AGU* **83**(47) Fall Meeting Supplement: Abstract H12F-09.

Sklar LS, Dietrich WE. 2004. A mechanistic model for river incision into bedrock by saltating bed load. *Water Resources Research* **40**: W06301. DOI: 10.1029/2003WR002496

Sklar LS, Dietrich WE. 2006. The role of sediment in controlling steady-state bedrock channel slope: implications of the saltation-abrasion incision model. *Geomorphology* **82**: 58–83.

Springer GS, Tooth S, Wohl EE. 2005. Dynamics of pothole growth as defined by field data and geometrical description. *Journal of Geophysical Research-Earth Surface* **110**: F04010. DOI: 10.1029/2005JF000321

Springer GS, Wohl EE. 2002. Empirical and theoretical investigations of sculpted forms in Buckeye Creek Cave, West Virginia. *Journal of Geology* **110**: 469–481.

Stark CP. 2006. A self-regulating model of bedrock river channel geometry. *Geophysical Research Letters* **33**: L04402. DOI: 10.1029/2005GL023193

Stark CP, Stark GJ. 2001. A channelization model of landscape evolution. *American Journal of Science* **301**: 486–512.

Stock JD, Montgomery DR, Collins BD, Dietrich WE, Sklar L. 2005. Field measurements of incision rates following bedrock exposure: implications for process controls on the long profiles of valleys cut by rivers and debris flows. *Geological Society of America Bulletin* **117**(1/2): 174–194.

Tinkler KJ, Parish, J. 1998. Recent adjustments to the long profile of Cooksville Creek, and urbanized bedrock channel in Mississauga, Ontario. In *Rivers Over Rock: Fluvial Processes in Bedrock Channels*, Tinkler K, Wohl EE (eds), American Geophysical Union Geophysical Monograph **107**: 167–187.

Tomkin JH, Brandon MT, Pazzaglia FJ, Barbour JR, Willett SD. 2003. Quantitative testing of bedrock incision models, Clearwater River, NW Washington State. *Journal of Geophysical Research*, **108** (B6): 2308. DOI: 10.1029/2001JB000862

van der Beek P, Bishop P. 2003. Cenozoic river profile development in the Upper Lachlan catchment (SE Australia) as a test of quantitative fluvial incision models. *Journal of Geophysical Research – Solid Earth* **108**(B6). DOI: 10.1029/2002JB002125

Whipple KX. 2004. Bedrock rivers and the geomorphology of active orogens. *Annual Review of Earth and Planetary Sciences* **32**: 151–185.

Whipple KX, Hancock G, Anderson RS. 2000. River incision into bedrock: mechanics and relative efficacy of plucking, abrasion, and cavitation. *Geological Society of America Bulletin* **112**: 490–503.

Whipple KX, Tucker GE. 1999. Dynamics of the stream-power river incision model: implications for height limits of mountain ranges, landscape response timescales, and research needs. *Journal of Geophysical Research – Solid Earth* **104**(B8): 17 661–17 674.

Whipple KX, Tucker GE. 2002. Implications of sediment-flux-dependent river incision models for landscape evolution. *Journal of Geophysical Research-Solid Earth* **107**(B2): art. No. 2039.

Willett SD. 1999. Orogeny and orography: the effects of erosion on the structure of mountain belts. *Journal of Geophysical Research – Solid Earth* **104**(B12): 28 957–28 981.

Wohl EE. 1992. Bedrock benches and boulder bars: floods in the Burdekin Gorge of Australia. *Geological Society of America Bulletin* **104**: 770–778.

Wohl EE. 1993. Bedrock channel incision along Piccaninny Creek, Australia. *Journal of Geology* **101**: 749–761.

Wohl EE. 1998. Bedrock channel morphology in relation to erosional processes. In *Rivers over Rock; Fluvial Processes in Bedrock Channels*, Tinkler KJ, Wohl EE (eds), American Geophysical Union Geophysical Monograph 107: 237–260.

Wohl EE, Ikeda H. 1997. Experimental simulation of channel incision into a cohesive substrate at varying gradients. *Geology* **25**: 295–298.

Wohl EE, Thompson DM, Miller AJ. 1999. Canyons with undulating walls. *Geological Society of America Bulletin* **111**: 949–959.

Zen EA, Prestegaard KL. 1994. Possible hydraulic significance of 2 kinds of potholes – examples from the Paleo-Potomac River. *Geology* **22**: 47–50.